Article

Cell Reports

Neutrophil-Derived IL-1β Impairs the Efficacy of NF-κB Inhibitors against Lung Cancer

Graphical Abstract

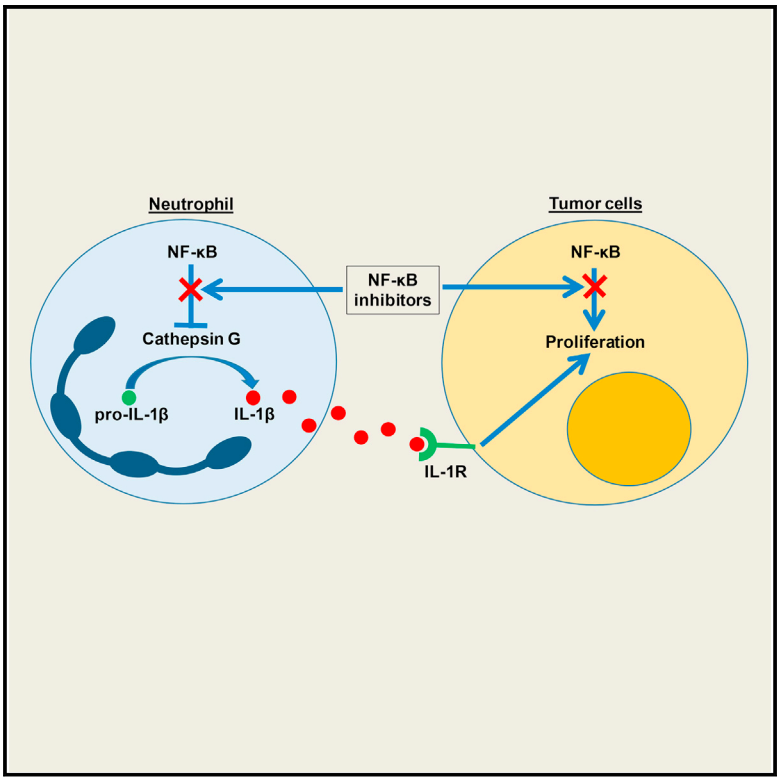

Authors

Allyson G. McLoed, Taylor P. Sherrill, Dong-Sheng Cheng, ..., Vassilis Georgoulias, Rinat Zaynagetdinov, Timothy S. Blackwell

Correspondence

rinat.z.zaynagetdinov@vanderbilt.edu

In Brief

McLoed et al. show that inhibition of NF-κB signaling in myeloid cells augments lung tumorigenesis. Myeloid-specific or systemic NF-κB inhibition increases IL-1β production by neutrophils, which enhances lung tumor formation. These studies highlight an important resistance pathway that limits efficacy of NF-κB inhibitors.

Highlights

- Inhibition of NF-κB signaling in myeloid cells enhances lung tumorigenesis
- Carcinogen treatment induces IL-1β processing in neutrophils with NF-κB inhibition
- NF-κB targeting with bortezomib increases IL-1β production in NSCLC patients
- Combination therapy with bortezomib and IL-1R antagonist slows tumor growth in mice

McLoed et al., 2016, Cell Reports *16*, 120–132
June 28, 2016
http://dx.doi.org/10.1016/j.celrep.2016.05.085

CellPress

OPEN ACCESS
CellPress

Cell Reports
Article

Neutrophil-Derived IL-1β Impairs the Efficacy of NF-κB Inhibitors against Lung Cancer

Allyson G. McLoed,[1] Taylor P. Sherrill,[2] Dong-Sheng Cheng,[2] Wei Han,[2] Jamie A. Saxon,[1] Linda A. Gleaves,[2] Pingsheng Wu,[3] Vasiliy V. Polosukhin,[2] Michael Karin,[4] Fiona E. Yull,[1,5] Georgios T. Stathopoulos,[2,6,7] Vassilis Georgoulias,[8] Rinat Zaynagetdinov,[2,11,*] and Timothy S. Blackwell[1,2,5,9,10,11]

[1]Department of Cancer Biology, Vanderbilt University, Nashville, TN 37232, USA
[2]Department of Medicine, Division of Allergy, Pulmonary and Critical Care Medicine, Vanderbilt University, Nashville, TN 37232, USA
[3]Department of Biostatistics, Vanderbilt University, Nashville, TN 37232, USA
[4]Laboratory of Gene Regulation and Signal Transduction, Departments of Pharmacology and Pathology, School of Medicine, University of California, San Diego, La Jolla, CA 92093, USA
[5]Vanderbilt-Ingram Cancer Center, 691 Preston Building, 2220 Pierce Ave., Nashville, TN 37232, USA
[6]Laboratory for Molecular Respiratory Carcinogenesis, Department of Physiology, University of Patras, Rio, 26504 Patras, Greece
[7]Comprehensive Pneumology Center (CPC), University Hospital, Ludwig-Maximilians University and Helmholtz Zentrum München, Member of the German Center for Lung Research (DZL), Munich 81377, Germany
[8]Department of Medical Oncology, University General Hospital of Heraklion, Heraklion, Crete 71110, Greece
[9]U.S. Department of Veterans Affairs, Washington, DC 20420, USA
[10]Department of Cell and Developmental Biology, Vanderbilt University, Nashville, TN 37232 USA
[11]Co-senior author
*Correspondence: rinat.z.zaynagetdinov@vanderbilt.edu
http://dx.doi.org/10.1016/j.celrep.2016.05.085

SUMMARY

Although epithelial NF-κB signaling is important for lung carcinogenesis, NF-κB inhibitors are ineffective for cancer treatment. To explain this paradox, we studied mice with genetic deletion of IKKβ in myeloid cells and found enhanced tumorigenesis in $Kras^{G12D}$ and urethane models of lung cancer. Myeloid-specific inhibition of NF-κB augmented pro-IL-1β processing by cathepsin G in neutrophils, leading to increased IL-1β and enhanced epithelial cell proliferation. Combined treatment with bortezomib, a proteasome inhibitor that blocks NF-κB activation, and IL-1 receptor antagonist reduced tumor formation and growth in vivo. In lung cancer patients, plasma IL-1β levels correlated with poor prognosis, and IL-1β increased following bortezomib treatment. Together, our studies elucidate an important role for neutrophils and IL-1β in lung carcinogenesis and resistance to NF-κB inhibitors.

INTRODUCTION

The nuclear factor κB (NF-κB) pathway has become increasingly appreciated for its involvement in carcinogenesis, as studies continue to uncover its roles in primary tumor growth, angiogenesis, and metastasis (Lin et al., 2010). In the lungs, NF-κB is activated in pre-malignant airway epithelial lesions, atypical adenomatous hyperplasia (AAH) lesions in the distal lungs, and invasive non-small-cell lung cancer (NSCLC) (Tichelaar et al., 2005). Based on this information, inhibition of the NF-κB pathway has been tested as a therapy for lung cancer (Chen et al., 2011). The proteasome inhibitor bortezomib, which blocks degradation of the inhibitor of NF-κB (IκB), as well as other proteins that are regulated by the proteasome, is the best-studied agent for inhibiting NF-κB in humans; however, bortezomib has not been efficacious for NSCLC treatment (Besse et al., 2012; Fanucchi et al., 2006). The mechanism of resistance to bortezomib and other NF-κB inhibitor therapies is not known. Despite the disappointing results to date, numerous clinical trials have been attempted, or are currently underway, to test various combinations of bortezomib and other agents for cancer treatment. Our goals for these studies were to determine why NF-κB inhibitors are ineffective for NSCLC and to identify new approaches to overcome resistance to NF-κB inhibitors.

Our group and others have shown that NF-κB signaling in lung epithelial cells is crucial for lung tumor formation. In mice, expression of a constitutively active form of IKKβ (which activates canonical NF-κB) in airway epithelium results in a >3-fold increase in lung tumor formation after treatment with chemical carcinogens (Zaynagetdinov et al., 2012). In addition, studies using a variety of methods to block NF-κB signaling in lung epithelium have revealed a requirement for NF-κB signaling in lung cancer models driven by oncogenic forms of Kras and EGFR (Bassères et al., 2010; Meylan et al., 2009; Saxon et al., 2016; Stathopoulos et al., 2007; Xia et al., 2012). While some studies have shown short-term lung tumor regression following NF-κB inhibition (Bassères et al., 2014; Xue et al., 2011), pharmacologic NF-κB inhibition has not shown definitive long-term benefit in lung cancer models. Highlighting the challenges of NF-κB inhibition, Xue et al. (2011) showed that murine lung tumors developed resistance to therapy within a few weeks after treatment with bortezomib or an inhibitor of IκBα phosphorylation (BAY 11-7082). Additionally, we showed that prolonged

treatment with bortezomib enhanced, not hindered, lung tumor formation in urethane-treated mice (Karabela et al., 2012). While it is possible that tumor cells could develop intrinsic resistance to NF-κB inhibitors via the acquisition of additional mutations (Xue et al., 2011), this would likely translate into the sporadic appearance of secondary resistance, as opposed to the uniform primary resistance, to bortezomib observed in solid tumors (Besse et al., 2012; Fanucchi et al., 2006). Based on these observations, we postulated that systemic NF-κB inhibition evokes a pro-tumorigenic response from a non-epithelial cell population that overrides the anti-tumor effects resulting from NF-κB inhibition in epithelial cells.

Myeloid cells play important roles in both innate immunity and tumorigenesis (Giannou et al., 2015; Stathopoulos et al., 2010; Zaynagetdinov et al., 2011). It is now well accepted that macrophages and neutrophils can act as pro- or anti-tumorigenic cells during tumorigenesis, depending on signals that they receive from the tumor and the tumor stroma (Fridlender and Albelda, 2012; Rajnavolgyi et al., 2013). The role of NF-κB signaling in these cells during tumorigenesis is controversial and seems to be organ and/or context dependent. Some cancer models show that blocking NF-κB signaling in myeloid cells elicits a protective, anti-tumorigenic response (Greten et al., 2004; Takahashi et al., 2010). Others show that myeloid-specific NF-κB inhibition is detrimental and pro-tumorigenic (Enzler et al., 2011; Yang et al., 2014). In tumor-associated macrophages, blocking NF-κB can result in an anti-tumorigenic phenotype (Fong et al., 2008; Hagemann et al., 2008). On the other hand, a recent study showed that blocking NF-κB signaling in macrophages impedes their ability to mount anti-tumorigenic responses against melanoma cells (Yang et al., 2014).

For these studies, we postulated that inhibition of NF-κB signaling in myeloid cells could elicit pro-tumorigenic responses that limit the effectiveness of global (systemic) NF-κB inhibition. To test this hypothesis, we utilized a mouse model characterized by myeloid cell-specific deletion of IKKβ (IKKβ$^{\Delta mye}$ mice; LysM-Cre/IKKβ$^{flox/flox}$) (Li et al., 2003). In carcinogen-induced and genetic lung cancer models, we found that blocking NF-κB signaling in myeloid cells enhances lung tumorigenesis through neutrophil-dependent production of interleukin (IL)-1β and that combined NF-κB and IL-1β targeted treatments reduces tumor formation and growth.

RESULTS

Neutrophils Enhance Lung Tumorigenesis when NF-κB Activity Is Inhibited in Myeloid Cells

To determine the role of NF-κB signaling in myeloid cells during lung tumorigenesis, IKKβ$^{\Delta mye}$ mice were fully backcrossed (more than nine generations) to the tumor-susceptible FVB background. Deletion of IKKβ in myeloid cells in the bone marrow compartment was confirmed by western blot (Figure S1). Subsequently, IKKβ$^{\Delta mye}$ mice and wild-type (WT) littermate controls were given a single intraperitoneal (i.p.) injection of the carcinogen urethane (1 g/kg). Urethane causes lung tumors primarily through the induction of *Kras* mutations (You et al., 1989), but it can also induce a number of other driver mutations found in human cancers (Westcott et al., 2015). At week 16 after injection of urethane, we found that IKKβ$^{\Delta mye}$ mice developed approximately twice as many lung tumors as WT mice (Figures 1A and 1B), indicating that inhibiting NF-κB signaling in myeloid cells promotes lung tumorigenesis. To determine whether differences were detectable at an earlier stage of carcinogenesis, we harvested lungs at 6 weeks after urethane injection and identified a greater number of AAH lesions in lungs of IKKβ$^{\Delta mye}$ mice compared to WT mice (Figure 1D). Unexpectedly, at 6 weeks post-urethane injection, we observed some fully formed tumors in the lungs of IKKβ$^{\Delta mye}$ mice (Figure 1C). On lung sections, 58% (7/12) of IKKβ$^{\Delta mye}$ lungs contained adenomas at 6 weeks post-urethane compared with 7.1% (1/14) of WT lungs ($p < 0.01$ by Fisher's exact test). To investigate the mechanism of enhanced tumorigenesis in IKKβ$^{\Delta mye}$ mice, we performed immunohistochemistry for markers of proliferation (PCNA) and apoptosis (cleaved caspase-3). Although we did not observe any differences in cleaved caspase-3 staining between IKKβ$^{\Delta mye}$ and WT lungs, there were significantly more PCNA^{+} lung epithelial cells in IKKβ$^{\Delta mye}$ mice compared to WT mice (Figures 1E and 1F; data not shown). To corroborate our findings from the urethane model, we utilized the LSL-Kras^{G12D} (Kras^{G12D}) lung tumor model (Tuveson et al., 2004). We performed bone marrow transplantation in Kras^{G12D} mice, using either WT (WT → Kras^{G12D}) or IKKβ$^{\Delta mye}$ (IKKβ$^{\Delta mye}$ → Kras^{G12D}) donors. Lung tumors were induced in these bone marrow chimeras by intratracheal (i.t.) instillation of adenoviral vectors expressing Cre recombinase (adeno-Cre). Similar to urethane-injected IKKβ$^{\Delta mye}$ mice, IKKβ$^{\Delta mye}$ → Kras^{G12D} mice developed twice as many lung tumors as WT → Kras^{G12D} mice at 8 weeks after adeno-Cre treatment (Figures 1G and 1H). Together, these studies show that blocking NF-κB signaling in myeloid cells promotes lung tumorigenesis in both chemical and genetic models of lung cancer.

Since NF-κB is an important regulator of inflammation, we next investigated the role of myeloid NF-κB signaling on lung inflammation during tumorigenesis. No differences in inflammatory cells in bronchoalveolar lavage (BAL) fluid were observed between untreated WT and IKKβ$^{\Delta mye}$ mice; however, at 6 weeks post-urethane injection, we observed increased inflammatory cells in BAL from IKKβ$^{\Delta mye}$ mice, indicating that heightened lung inflammation in IKKβ$^{\Delta mye}$ mice was an effect of carcinogen treatment (Figure 2A). To evaluate specific myeloid subpopulations, we performed flow cytometry on lung cells from IKKβ$^{\Delta mye}$ and WT mice (Figure 2B). Consistent with findings in BAL, no differences in neutrophil, monocyte, or macrophage cell populations were observed between untreated WT and IKKβ$^{\Delta mye}$ mice (Figure 2C). In contrast, we identified a selective increase in neutrophils in the lungs of IKKβ$^{\Delta mye}$ mice at 6 weeks post-urethane injection, compared to WT mice, but no difference in total CD45^{+} cells (Figures 2D and S2). Additional studies in Kras^{G12D} model bone marrow chimeras showed similar findings with increased lung neutrophils in IKKβ$^{\Delta mye}$ → Kras^{G12D} mice at 8 weeks after i.t. adeno-Cre instillation compared to WT → Kras^{G12D} mice (Figures 2E and 2F).

In order to determine whether neutrophils were important for lung carcinogenesis, we performed neutrophil depletion using antibodies against Ly6G (Fleming et al., 1993). WT and IKKβ$^{\Delta mye}$ mice were injected with urethane and administered anti-Ly6G antibodies or isotype control immunoglobulin G (IgG) antibodies

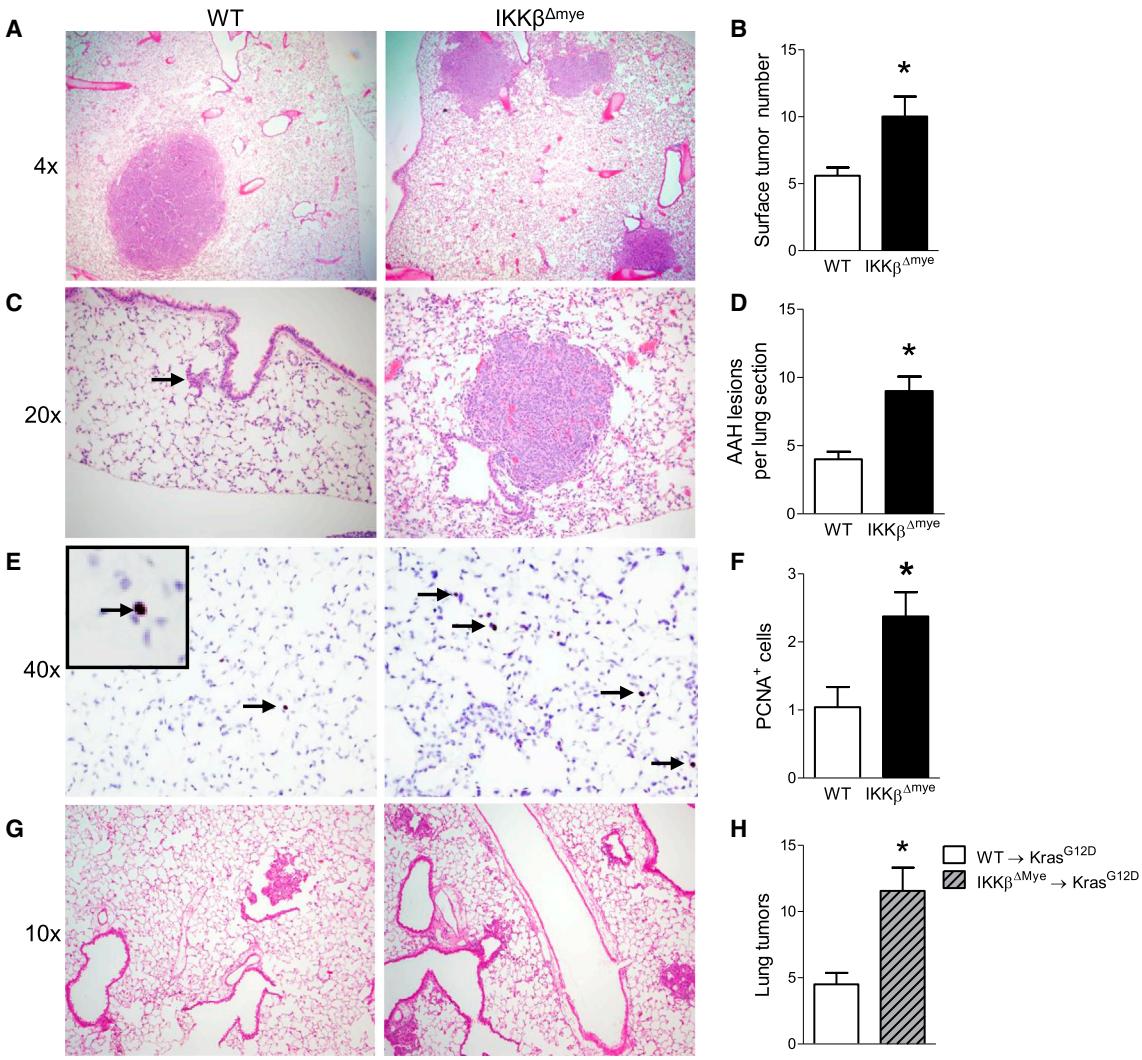

Figure 1. Inhibition of NF-κB Signaling in Myeloid Cells Increases Lung Tumorigenesis and Epithelial Cell Proliferation

(A and B) Representative photomicrographs (A) and number of lung tumors (B) in WT and IKKβ$^{\Delta mye}$ mice at 16 weeks after a single injection of urethane (n = 16–22 mice per group).

(C) Representative photomicrographs showing an AAH lesion (red arrow) in the lung of WT mice or tumor in IKKβ$^{\Delta mye}$ mice.

(D) Number of AAH lesions counted per H&E-stained lung sections (three sections per mouse) from WT and IKKβ$^{\Delta mye}$ mice harvested at week 6 after injection of urethane (n = 9–10 mice per group).

(E and F) Immunostaining for PCNA^{+} cells (E) and number of PCNA^{+} cells per lung section (F) (averaged from 25 sequential fields taken at 40× magnification) from WT and IKKβ$^{\Delta mye}$ mice harvested at week 6 after urethane injection (n = 3–4 per group).

(G and H) Lethally irradiated LSL-Kras^{G12D} mice received bone marrow from WT (WT → Kras^{G12D}) or IKKβ$^{\Delta mye}$ (IKKβ$^{\Delta mye}$ → Kras^{G12D}) mice. Lung tumors were induced by instillation of i.t. adeno-Cre (1.5×10^{7} PFU). Representative photomicrographs (G) and number of lung tumors (H) in WT → Kras^{G12D} and IKKβ$^{\Delta mye}$ → Kras^{G12D} mice at 8 weeks after adeno-Cre (n = 4–9 mice per group).

Error bars indicate mean ± SEM. *$p < 0.05$.

See also Figure S1.

(100 μg) twice weekly for 6 weeks. A marked reduction in lung neutrophils was confirmed by flow cytometry (Figures 3A and 3B). While neutrophil depletion significantly reduced AAH lesions in the lungs of IKKβ$^{\Delta mye}$ mice, we observed no effect of this treatment in WT mice (Figure 3C). Next, we tested the effect of neutrophil depletion on lung tumor formation. A bone marrow transplantation study was incorporated into this experiment to verify that enhanced tumorigenesis in IKKβ$^{\Delta mye}$ mice following urethane treatment was due to bone-marrow-derived leukocytes. Lethally irradiated WT mice received bone marrow from IKKβ$^{\Delta mye}$ (IKKβ$^{\Delta mye}$ → WT) or WT (WT → WT) donors. Bone marrow chimeras were injected with urethane and administered anti-Ly6G antibodies or isotype control IgG antibodies (100 μg) twice weekly for 6 weeks. At week 16 after urethane injection, we observed increased tumor formation in the lungs of control (IgG-treated) IKKβ$^{\Delta mye}$ → WT mice compared to control

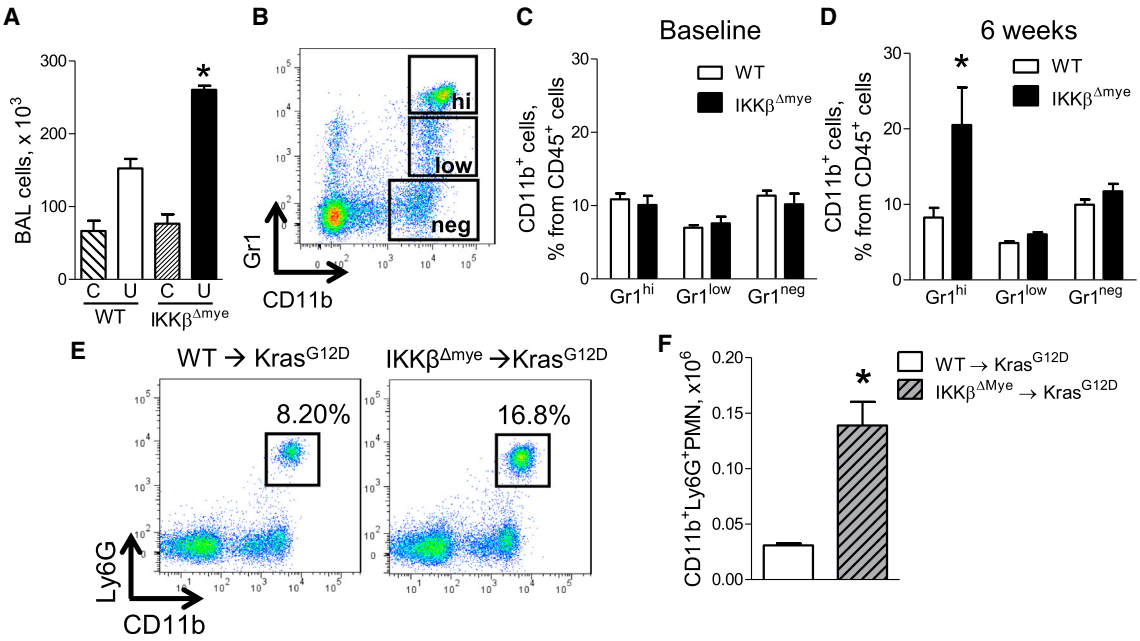

Figure 2. Neutrophils Are Increased in the Lungs of Mice Lacking Myeloid NF-κB Signaling

(A) Number of total BAL cells in WT and IKKβ$^{\Delta mye}$ mice at baseline (C) and at 6 weeks after urethane injection (U) (n = 7–9 mice per group; *p < 0.05, compared with urethane-treated WT mice).

(B–D) Representative fluorescence-activated cell sorting (FACS) plots (B) and percentages of viable CD45$^+$/CD11b$^+$/Gr1^{hi} neutrophils (Gr1^{hi}), CD45$^+$/CD11b$^+$/Gr1^{low} monocytes (Gr1^{low}), and CD45$^+$/CD11b$^+$/Gr1^{neg} macrophages (Gr1^{neg}) in the lungs of WT and IKKβ$^{\Delta mye}$ mice at baseline (C) and 6 weeks after urethane injection (D) (n = 4–11 mice per group; *p < 0.05, compared with WT).

(E and F) Representative FACS plots (E) and total viable CD45$^+$/CD11b$^+$/Ly6G$^+$ neutrophils (F) in the lungs of WT → Kras^{G12D} and IKKβ$^{\Delta mye}$ → Kras^{G12D} mice 8 weeks after adeno-Cre (n = 4 mice per group; *p < 0.05, compared with WT → Kras^{G12D}). Ly6G identifies the granulocytic subgroup of the Gr1 marker.

Error bars indicate mean ± SEM.

See also Figure S2.

(IgG-treated) WT → WT mice (Figure 3D). In addition, neutrophil depletion using anti-Ly6G antibodies significantly reduced tumor formation in IKKβ$^{\Delta mye}$ → WT mice, compared to control (IgG-treated) IKKβ$^{\Delta mye}$ → WT mice, identifying neutrophils as key mediators of increased tumor formation in the setting of myeloid NF-κB inhibition.

Myeloid-Specific NF-κB Inhibition Results in Increased IL-1β Production by Neutrophils following Carcinogen Exposure

To determine how IKKβ-deficient neutrophils exert their pro-tumorigenic effects during lung carcinogenesis, we characterized neutrophils from IKKβ$^{\Delta mye}$ and WT mice according to morphological appearance, maturity, and function. We sorted neutrophils (CD45$^+$/CD11b$^+$/Ly6C$^+$/Ly6G$^+$ cells, hereafter referred to as Ly6G$^+$ cells) from lungs of urethane-treated IKKβ$^{\Delta mye}$ and WT mice and confirmed that these cells had segmented nuclei, characteristic of mature neutrophils (Figure 4A). As early as 1 week after urethane injection, IKKβ$^{\Delta mye}$ mice had an approximately 3-fold increase in neutrophils in the lungs, compared to WT mice, while lung monocytes (CD45$^+$/CD11b$^+$/Ly6C$^+$/Ly6G$^-$ cells) and macrophages (CD45$^+$/CD11b$^+$/Ly6C$^-$/Ly6G$^-$ cells), as well as peripheral blood neutrophils, were comparable between groups (Figure 4B; data not shown). To determine whether loss of NF-κB signaling affected maturation of neutrophils, we measured the expression of myeloperoxidase (MPO), an enzyme produced by mature neutrophils, in Ly6G$^+$ cells from IKKβ$^{\Delta mye}$ and WT mice at 1 week after urethane injection (Figure 4C). Loss of NF-κB signaling in Ly6G$^+$ cells from IKKβ$^{\Delta mye}$ mice did not impair MPO production (Figures 4C and 4D). We also examined N1/N2 markers in lung neutrophils by real-time PCR but did not observe differences in anti-tumorigenic N1 markers (TNFα, IL-12p35, ICAM1, IFNγ, and iNOS) or pro-tumorigenic N2 markers (CCL2, CCL5, CCL17, VEGF, IL-10, and Arg1) between neutrophils from urethane-injected WT and IKKβ$^{\Delta mye}$ mice (Figures 4E and 4F). Since a subset of Ly6G$^+$ cells (granulocytic myeloid-derived suppressor cells [MDSCs]) may support tumorigenesis through suppression of anti-tumor responses from T lymphocytes (Gabrilovich and Nagaraj, 2009), we assessed the ability of Ly6G$^+$ cells isolated from lungs of urethane-treated IKKβ$^{\Delta mye}$ mice to suppress effector T (Teff) cell proliferation in an allogeneic mixed-lymphocyte reaction assay. As shown in Figure 4G, Ly6G$^+$ cells from IKKβ$^{\Delta mye}$ mice failed to suppress proliferation of Teff cells stimulated by allogeneic dendritic cells, indicating that Ly6G$^+$ cells from IKKβ$^{\Delta mye}$ mice do not act as MDSCs. These studies show that neutrophils from IKKβ$^{\Delta mye}$ mice are mature cells that are not highly polarized toward N1 or N2 and do not exhibit immunosuppressive properties during early lung tumorigenesis.

Since we did not identify differences in maturation or function of neutrophils from IKKβ$^{\Delta mye}$ mice, we investigated whether differential production of inflammatory mediators could be responsible for

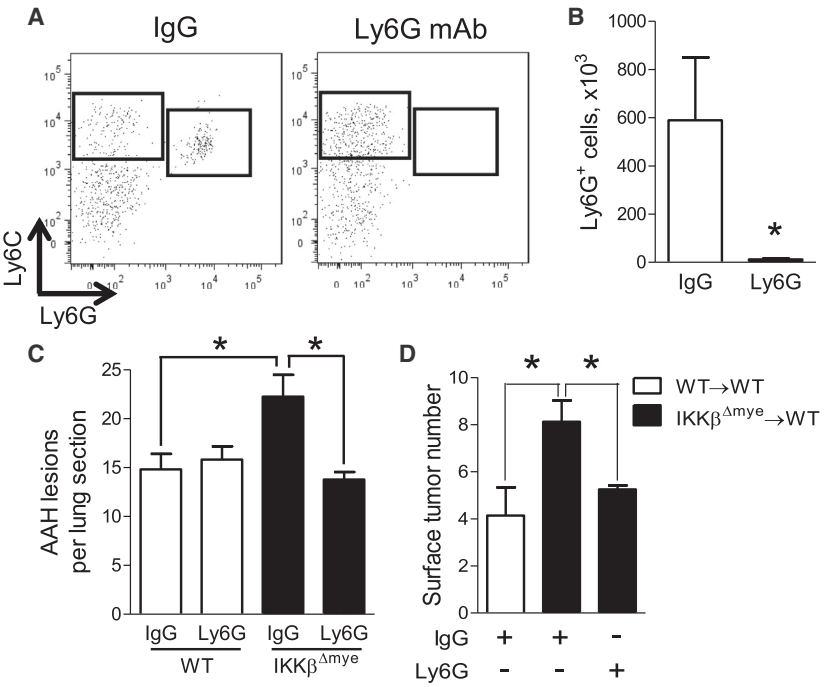

Figure 3. Neutrophils Promote Lung Tumorigenesis in the Absence of Myeloid NF-κB Signaling

All mice were treated with isotype control IgG or anti-Ly6G depletion antibodies (100 μg by i.p. injection) for the first 6 weeks following urethane injection.

(A and B) Representative FACS plots (A) and total viable $CD45^+/CD11b^+/Ly6C^+/Ly6G^+$ lung neutrophils (B), demonstrating depletion efficiency in $IKK\beta^{\Delta mye}$ mice analyzed 3 days after the last dose of antibody (n = 4 mice per group). mAb, monoclonal antibody.

(C) Number of AAH lesions per lung section from IgG- and anti-Ly6G-treated WT and $IKK\beta^{\Delta mye}$ mice at 6 weeks after urethane injection (n = 6–9 mice per group).

(D) Lethally irradiated WT mice received bone marrow from WT or $IKK\beta^{\Delta mye}$ mice. Lung tumors at 16 weeks after urethane injection in bone marrow of chimera mice treated with IgG or anti-Ly6G antibodies for the first 6 weeks of tumorigenesis (n = 6–8 mice per group).

Error bars indicate mean ± SEM. *$p < 0.05$.

increased tumorigenesis in the context of NF-κB inhibition. We measured mRNA and protein expression of a panel of cytokines (G-CSF, GM-CSF, IFNγ, IL-1β, IL-4, IL-6, IL-10, IL-12p40, KC, MCP-1, and MIP-1α) in the lungs of $IKK\beta^{\Delta mye}$ and WT mice at 1 week after urethane injection. Both KC mRNA and protein were increased in lungs of $IKK\beta^{\Delta mye}$ mice, while IL-1β protein, but not mRNA, was upregulated (Figures 5A and 5B). For IL-1β, increased protein without increased mRNA expression suggests increased pro-IL-1β processing. No differences in IL-1β protein levels in the lungs were detected between untreated WT and $IKK\beta^{\Delta mye}$ mice (data not shown). To determine the cellular source for increased IL-1β protein in $IKK\beta^{\Delta mye}$ mice, we sorted myeloid cells from lungs at 1 week after urethane injection and measured IL-1β in conditioned media. Neutrophils from $IKK\beta^{\Delta mye}$ mice secreted nearly twice as much IL-1β as monocytes or macrophages (Figure 5C) and produced more IL-1β per cell than lung neutrophils from urethane-injected WT mice (Figure 5D), identifying IKKβ-deficient neutrophils as the source of increased IL-1β protein levels in the lungs. To verify that neutrophils were the primary source of IL-1β, we performed macrophage and neutrophil depletion studies in urethane-treated $IKK\beta^{\Delta mye}$ mice. For macrophage depletion, urethane-treated $IKK\beta^{\Delta mye}$ mice were administered liposomal clodronate or vehicle (liposomal PBS) by i.t. injection (Zaynagetdinov et al., 2011) and lungs were harvested at 1 week after urethane. Macrophage depletion did not alter IL-1β protein in the lungs of $IKK\beta^{\Delta mye}$ mice (Figure 5E). For neutrophil depletion, urethane-treated $IKK\beta^{\Delta mye}$ mice received i.p. injections of 100 μg of anti-Ly6G or isotype control IgG antibodies (Chen et al., 2012; Fridlender et al., 2009), and lungs were harvested 1 week later. Neutrophil depletion in mice treated with anti-Ly6G antibodies was confirmed by flow cytometry (data not shown). Compared to $IKK\beta^{\Delta mye}$ mice treated with control IgG antibodies, anti-Ly6G antibody treatment significantly reduced IL-1β in the lungs (Figure 5F). Taken together, these studies point to IL-1β as a neutrophil-derived mediator that could support enhanced lung tumorigenesis.

Serine proteases have been implicated in the regulation of IL-1β processing by neutrophils (Greten et al., 2007); therefore, we performed inhibitor studies to determine the mechanism of dysregulated IL-1β release by lung neutrophils from $IKK\beta^{\Delta mye}$ mice. Lung neutrophils were isolated from urethane-treated WT and $IKK\beta^{\Delta mye}$ mice and cultured in the presence of inhibitors of caspase-1 (Ac-YVAD-CMK; YVAD), neutrophil elastase and proteinase 3 (MeOSuc-APPV-CMK; MeO), or cathepsin G (Z-GLP-CMK; GLP). While caspase-1 inhibition partially reduced IL-1β release from $IKK\beta^{\Delta mye}$ neutrophils, inhibition of the serine protease cathepsin G blocked nearly all IL-1β secretion (Figure 5G). Additionally, gene expression of cathepsin G was upregulated in lung neutrophils from urethane-treated $IKK\beta^{\Delta mye}$ mice, compared to WT mice, while no differences in expression were observed in caspase-1, neutrophil elastase, or proteinase 3 (Figure 5H; data not shown). These data implicate cathepsin G as the primary regulator of IL-1β processing by lung neutrophils in urethane-treated mice. Increased cathepsin G expression and/or activity in $IKK\beta^{\Delta mye}$ neutrophils likely accounts for the increased production of IL-1β by these cells.

Systemic NF-κB Inhibition Increases IL-1β Production in Mice and Humans with Lung Cancer

Next, we sought to determine whether IL-1β dysregulation could be detected following treatment with pharmacological NF-κB inhibitors in mice and human NSCLC patients. WT mice were treated with the proteasome inhibitor bortezomib (1 mg/kg) (Karabela et al., 2012; Xue et al., 2011) or vehicle by i.p. injection on days 2 and 6 following urethane injection, and analyzed on day 7 (Figure 6A). We observed elevated numbers of neutrophils in BAL from bortezomib-treated mice compared to vehicle-treated controls (Figure 6B). In addition, we found increased IL-1β protein

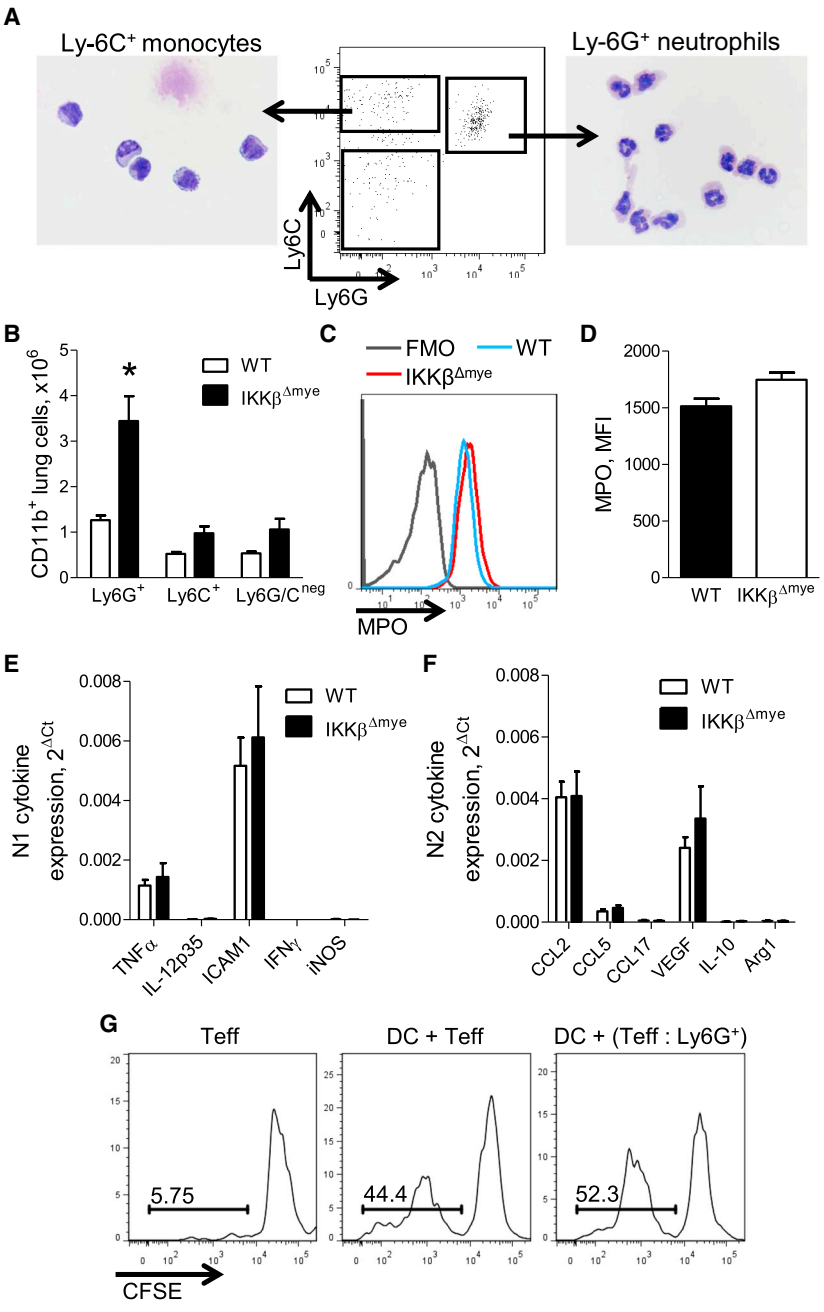

Figure 4. Mature Neutrophils Are Increased in the Lungs during Early Tumorigenesis in the Absence of Myeloid NF-κB Signaling

(A) FACS sorting strategy and photomicrographs demonstrating cell morphology of lung monocytes ($CD45^+/CD11b^+/Ly6C^+/Ly6G^-$) and neutrophils ($CD45^+/CD11b^+/Ly6C^+/Ly6G^+$) isolated from lungs of WT and $IKK\beta^{\Delta mye}$ mice at 1 week after urethane injection.

(B) Numbers of $CD11b^+/Ly6G^+$ neutrophils ($Ly6G^+$), $CD11b^+/Ly6C^+$ monocytes ($Ly6C^+$), and $CD11b^+/Ly6G^{neg}/Ly6C^{neg}$ macrophages ($Ly6G/C^{neg}$) in the lungs of WT and $IKK\beta^{\Delta mye}$ mice at 1 week after urethane injection (n = 3 mice per group, representative of two independent experiments; *$p < 0.05$, compared to WT).

(C and D) Flow cytometry plot (including fluorescence minus one [FMO] control) (C) and mean fluorescence intensity (MFI) (D) showing expression of MPO in viable $CD45^+/CD11b^+/Ly6G^+$ cells from lungs of WT and $IKK\beta^{\Delta mye}$ mice at 1 week after urethane injection (n = 4 mice per group).

(E and F) Expression of N1 (E) and N2 (F) markers in $CD45^+/CD11b^+/Ly6G^+$ cells isolated from lungs of $IKK\beta^{\Delta mye}$ mice at 1 week after urethane injection (n = 4–5 mice per group).

(G) $CD45^+/CD11b^+/Ly6G^+$ cells isolated from lungs of $IKK\beta^{\Delta mye}$ mice at 1 week after urethane injection do not impair the ability of allogeneic dendritic cells (DC) to induce proliferation of CFSE-labeled responder $CD4^+/CD25^-$ T cells (Teff) (1:1, performed in duplicate).

Error bars indicate mean ± SEM.

in both serum and lungs of bortezomib-treated mice compared to mice treated with vehicle (Figures 6C and 6D). To test whether these effects were common to different classes of NF-κB inhibitors, we repeated our studies using BAY 11-7082 (BAY). NF-κB inhibition was verified by luciferase activity as a measure of NF-κB activity in vehicle- or BAY-treated NF-κB reporter mice (Everhart et al., 2006) after urethane injection (Figure S3). At 1 week after urethane injection, BAY treatment resulted in increased neutrophils in BAL and lung tissue (Figures 6E–6G). BAY-treated mice also had elevated IL-1β protein in lung homogenates, compared to vehicle-treated mice, similar to $IKK\beta^{\Delta mye}$ mice (Figure 6H). Unlike $IKK\beta^{\Delta mye}$ mice, however, KC expression was not increased in BAY-treated WT mice (Figure S4).

To investigate the relevance of our mouse model findings to human NSCLC, we obtained blood samples from a completed study involving 28 chemotherapy-naive individuals with advanced stage (III–IV) NSCLC (protocol NCT01633645) (Table S1). In this study, patients received one cycle of bortezomib followed by a standard chemotherapy/bortezomib combination regimen. In plasma obtained before and 24 hr after the first dose of bortezomib (1 mg/m^2), we measured a panel of cytokines (IL-1β, IL-8, TNF, and IL-6) using cytometric bead array and found that treatment with bortezomib significantly increased IL-1β protein in the plasma of advanced NSCLC patients; however, no differences were detected in IL-8, TNF, or IL-6 (Figures 6I–6L). In addition, we found that, after controlling for age and performance status, IL-1β level at baseline significantly correlated with reduced progression-free survival in this cohort ($p = 0.026$) (Figure 6M).

IL-1β Promotes Lung Tumorigenesis, Enhances Epithelial Cell Proliferation, and Mediates Resistance to NF-κB Inhibitor Therapy

Since IL-1β production is increased in tumor models in the setting of myeloid and systemic NF-κB inhibition, we

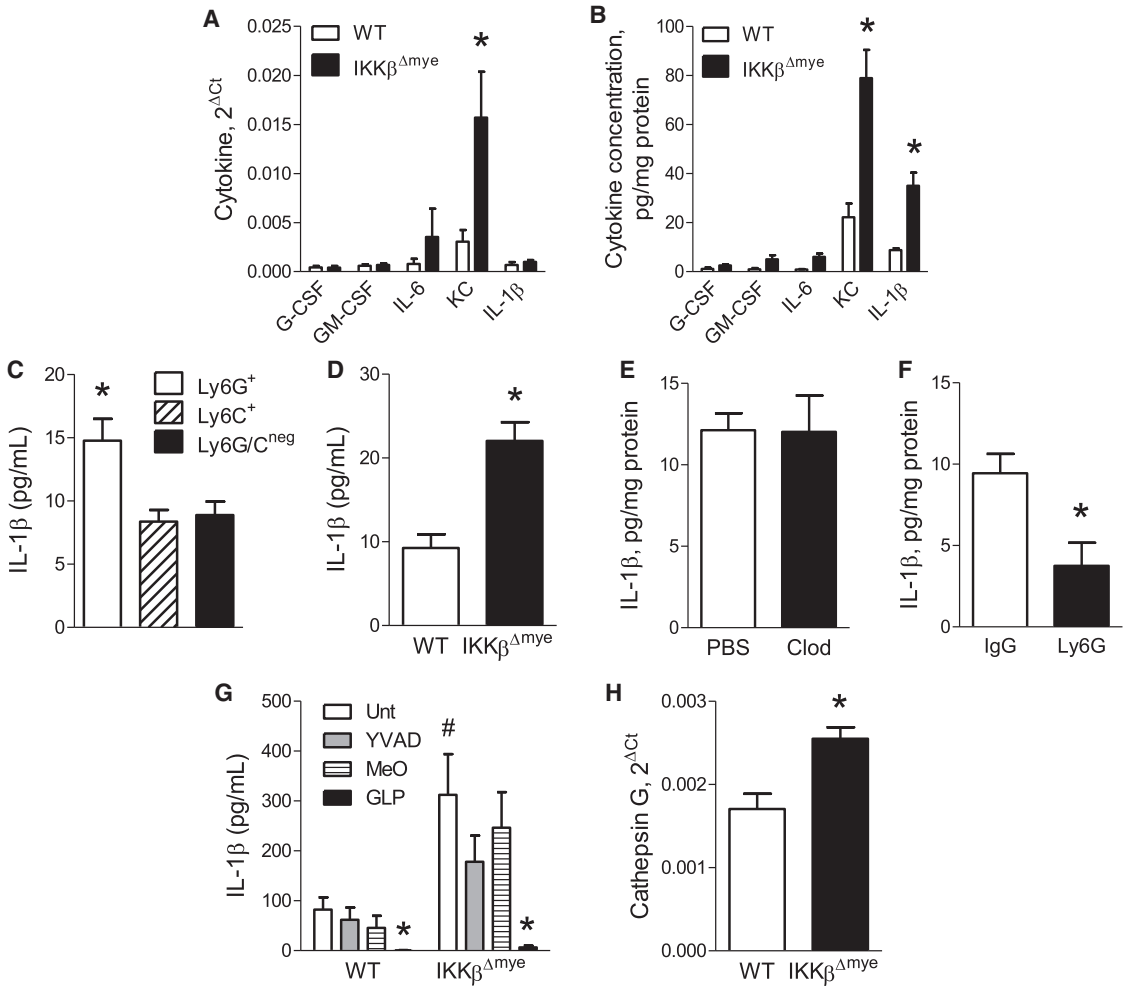

Figure 5. Neutrophils from IKKβ$^{\Delta mye}$ Mice Produce Increased IL-1β following Urethane Injection

(A and B) Expression of cytokines by (A) mRNA and (B) protein in the lungs of WT and IKKβ$^{\Delta mye}$ mice harvested 1 week after urethane (n = 10–11 mice per group; *p < 0.05, compared with WT).

(C) Concentration of IL-1β in the conditioned media following 12 hr culture of lung Ly6G$^+$ neutrophils, Ly6C$^+$ monocytes, or Ly6G/C^{neg} macrophages isolated from IKKβ$^{\Delta mye}$ mice at 1 week after urethane injection (n = 3; *p < 0.05, compared with Ly6C$^+$ and Ly6G/C^{neg}).

(D) Concentration of IL-1β in the conditioned media following 12 hr culture of equal numbers of lung Ly6G$^+$ neutrophils from WT and IKKβ$^{\Delta mye}$ mice isolated at 1 week after urethane injection (n = 8 mice per group). *p < 0.05.

(E) IL-1β protein levels in lung homogenates at 1 week after urethane in the lungs of IKKβ$^{\Delta mye}$ mice treated with liposomal clodronate (Clod) or PBS on day 5 following urethane injection (n = 6 mice per group).

(F) IL-1β protein levels at 1 week after urethane in the lungs of IKKβ$^{\Delta mye}$ mice treated with anti-Ly6G antibodies (100 μg) or control IgG antibodies by i.p. injection on days 1, 2, and 5 relative to the day of urethane injection (n = 3–5 mice per group; *p < 0.05, compared with IKKβ$^{\Delta mye}$ mice treated with control IgG antibodies). Lung Ly6G$^+$ neutrophils were isolated from WT and IKKβ$^{\Delta mye}$ mice at 1 week after urethane injection.

(G) IL-1β concentration in the conditioned media after culture with inhibitors (all, 100 μM) of caspase-1 (Ac-YVAD-CMK), neutrophil elastase and proteinase-3 (MeOSuc-APPV-CMK), or cathepsin G (Z-GLP-CMK) (n = 3–8 replicates per group; #p > 0.05, compared to WT untreated (Unt); *p < 0.05, compared to either WT or IKKβ$^{\Delta mye}$ Unt).

(H) mRNA expression of cathepsin G in lung Ly6G$^+$ neutrophils isolated from WT and IKKβ$^{\Delta mye}$ mice at 1 week after urethane injection. *p < 0.05.

Error bars indicate mean ± SEM.

investigated the impact of IL-1β on lung tumorigenesis using the clinically available IL-1 receptor antagonist (IL-1ra, anakinra/Kineret). IL-1ra (60 mg/kg/day) was delivered during the first 4 weeks after urethane injection to WT and IKKβ$^{\Delta mye}$ mice using subcutaneously implanted osmotic pumps (Figure 7A). Osmotic pumps filled with vehicle (PBS) were used as controls. As shown in Figure 7B, IL-1ra treatment significantly decreased the number of AAH lesions in the lungs of IKKβ$^{\Delta mye}$ mice at 6 weeks after urethane injection. To evaluate the impact of IL-1β signaling on tumor formation, we repeated these studies and harvested lungs from mice 16 weeks after urethane treatment. We found that IL-1ra treatment reduced lung tumors in IKKβ$^{\Delta mye}$ mice by more than 50% compared to IKKβ$^{\Delta mye}$ mice treated with vehicle (Figure 7C). Based on our finding that IKKβ$^{\Delta mye}$ mice have

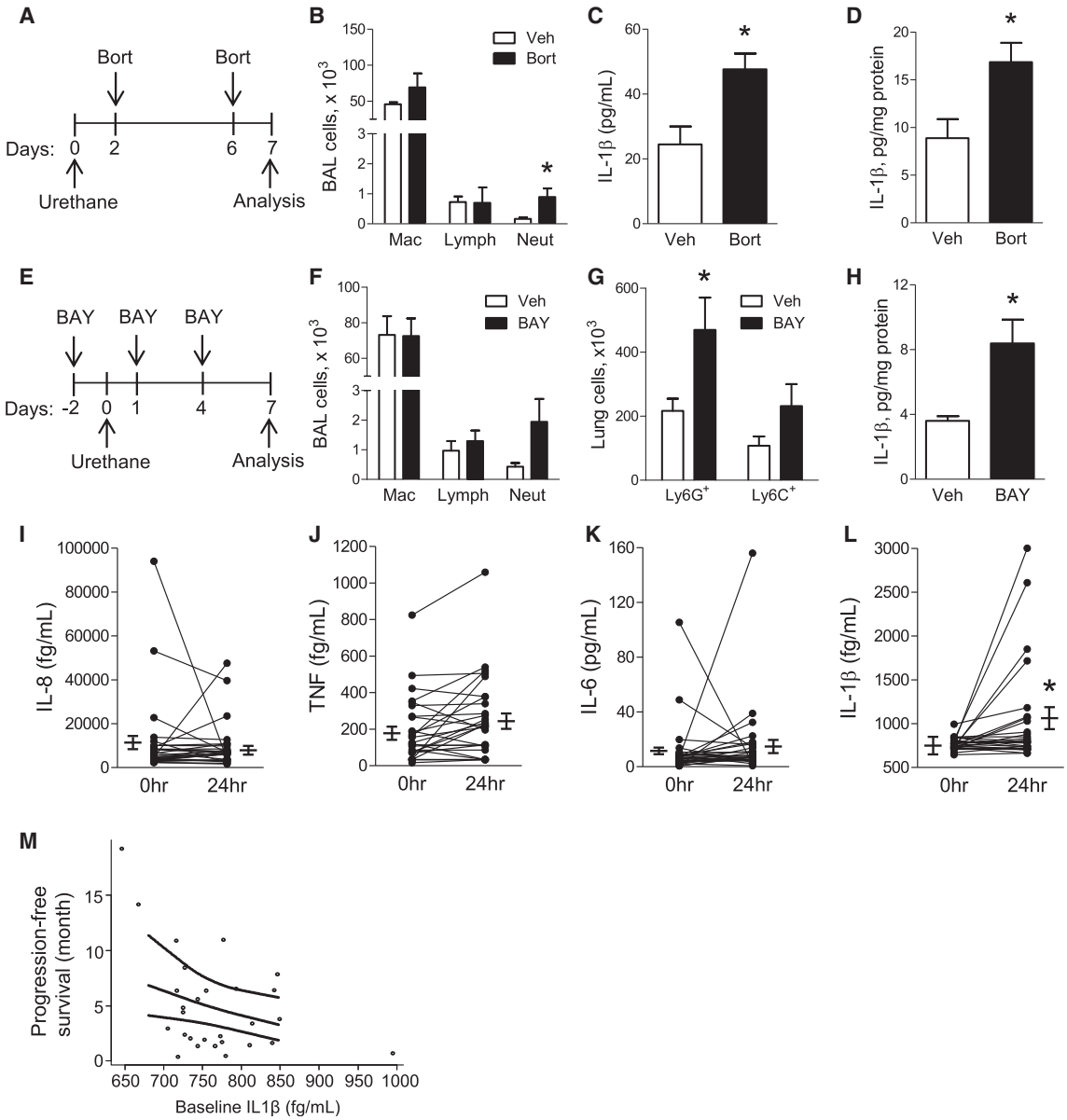

Figure 6. Pharmacological Inhibition of NF-κB Increases IL-1β in Mice and Indicates Worse Survival in NSCLC Patients

(A) Schematic representation of NF-κB inhibition protocol using bortezomib (Bort). In addition to urethane, WT mice were treated with i.p. injections of Bort (1 mg/kg) or vehicle control (Veh).

(B) BAL cells in Bort- or Veh-treated WT mice at 1 week after urethane injection (n = 4–5 mice per group; *p < 0.05, compared to Veh). Mac, macrophages; Neut, neutrophils; Lymph, lymphocytes.

(C and D) Serum (C) and lung (D) IL-1β protein levels from Bort- or Veh-treated WT mice 1 week after urethane (n = 6 mice per group). *p < 0.05.

(E) Schematic representation of the NF-κB inhibition protocol using BAY 11-7082 (BAY). In addition to urethane, WT mice were treated with i.p. injections of the specific NF-κB inhibitor BAY (10 mg/kg) or Veh.

(F) BAL cells in BAY- and Veh-treated WT mice at 1 week after urethane injection (n = 8 mice per group).

(G) Number of Ly6G$^+$ neutrophils and Ly6C$^+$ monocytes in the lungs of BAY- or Veh-treated mice at 1 week after urethane injection (n = 4–5 mice per group; *p < 0.05, compared to Veh).

(H) IL-1β protein levels in the lungs of BAY- or Veh-treated mice at 1 week after urethane injection (n = 8 mice per group). *p < 0.05.

(I–L) IL-8 (I), TNF (J), IL-6 (K), and IL-1β (L) protein levels in the plasma of NSCLC patients treated before (0hr) and 24 hr after treatment with bortezomib (1 mg/m^2) (n = 28 patients; *p < 0.05, compared with 0 hr).

(M) Correlation analysis between progression-free survival and baseline plasma IL-1β protein levels in advanced NSCLC patients treated with bortezomib plus standard chemotherapy (p = 0.026).

Error bars indicate mean ± SEM.

See also Figures S3 and S4 and Table S1.

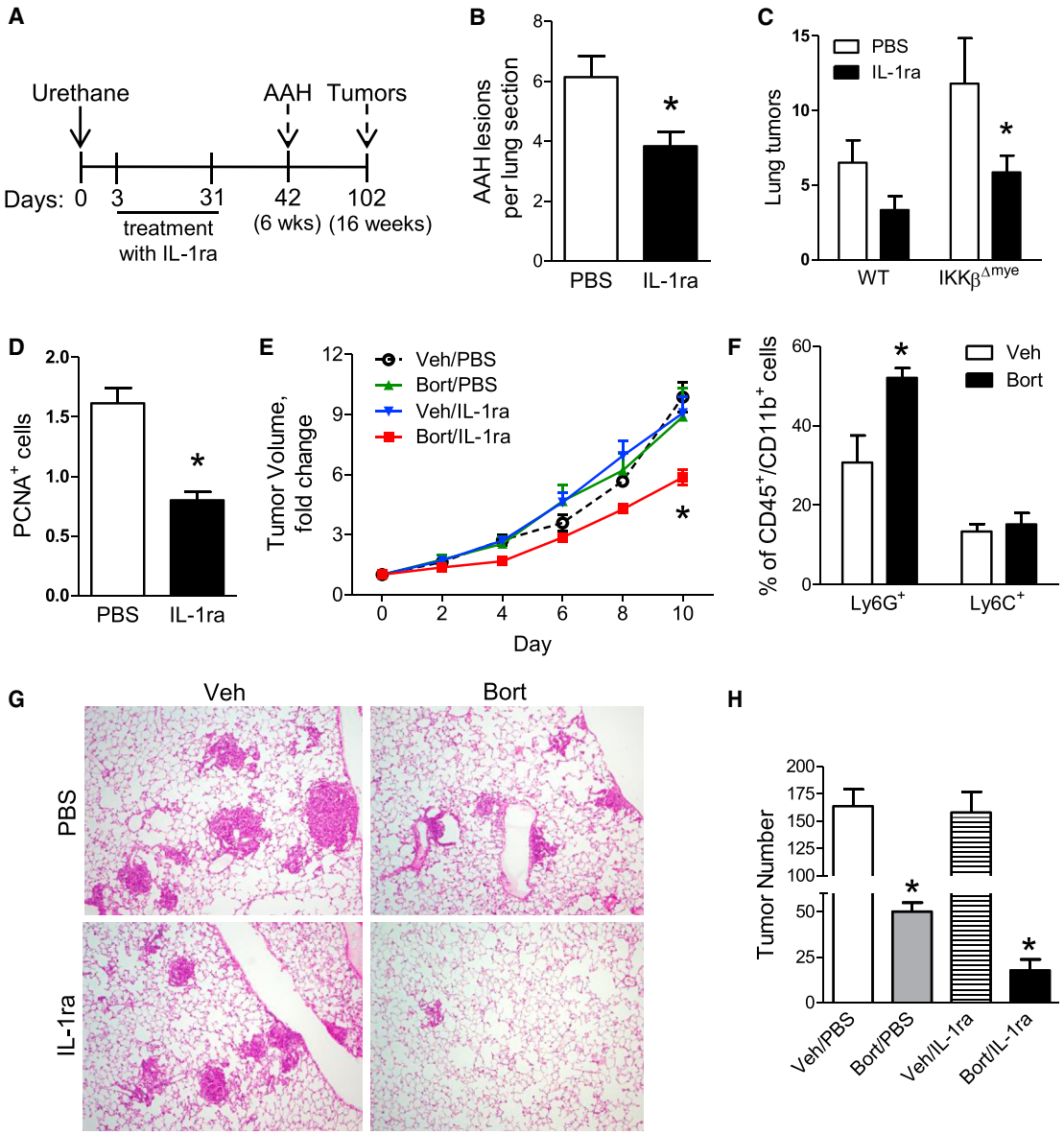

Figure 7. IL-1β Facilitates Lung Tumorigenesis by Stimulating Epithelial Cell Proliferation and Supports Resistance to Bortezomib Therapy

(A) Schematic representation of IL-1 receptor antagonist (IL-1ra) treatment protocol. WT and IKKβ$^{\Delta mye}$ mice were injected with a single dose of urethane and treated by osmotic pump delivery of 60 mg/kg/day of IL-1ra or PBS for the first 4 weeks.

(B) Number of AAH lesions per H&E-stained lung section harvested from IKKβ$^{\Delta mye}$ mice at week 6 after injection of urethane (n = 9 mice per group, *p < 0.05, compared with PBS).

(C) Lung tumors on H&E-stained lung sections from WT and IKKβ$^{\Delta mye}$ mice cut at predetermined depths (five sections per mouse, n = 7 mice per group; *p < 0.05, compared with PBS-treated IKKβ$^{\Delta mye}$ mice).

(D) Number of PCNA^{+} cells per lung section (averaged from 25 sequential fields taken at 40× magnification) from IKKβ$^{\Delta mye}$ mice harvested at week 6 after urethane injection (n = 9 mice per group; *p < 0.05, compared with PBS).

(E) Fold change of subcutaneous LLC tumor volume over 10 days of treatment with vehicle (Veh) control, bortezomib (Bort), IL-1ra, or Bort plus IL-1ra (n = 6–9 mice per group; *p < 0.05, compared with control).

(F–H) Inducible Kras^{G12D} mice were treated with doxycycline (dox) for 4 weeks to develop lung tumors. (F) Percentage of Ly6G^{+} and Ly6C^{+} cells in the lungs of dox-inducible Kras^{G12D} mice treated for 1 additional week with Bort or Veh plus dox (*p < 0.05, compared to Veh). (G) Representative photomicrographs and (H) numbers of surface lung tumors in mice treated with dox alone for 4 weeks, followed by 4 weeks of treatment with dox plus vehicle control, Bort, IL-1ra, or Bort plus IL-1ra (n = 6–7 mice per group; *p < 0.05, compared with control).

Error bars indicate mean ± SEM.

increased lung epithelial cell proliferation during tumorigenesis, we tested whether IL-1β could exert its pro-tumorigenic effects by altering proliferation of epithelial cells. We performed PCNA immunostaining on lung sections from IL-1ra- and PBS-treated IKKβ$^{\Delta mye}$ mice harvested 6 weeks after urethane and found reduced PCNA^{+} lung epithelial cells in IL-1ra-treated IKKβ$^{\Delta mye}$ mice (Figure 7D), demonstrating that IL-1β signaling supports epithelial cell proliferation during tumorigenesis. Together, these results indicate a pro-tumorigenic role for IL-1β in the setting of NF-κB inhibition in myeloid cells.

Since IL-1β is dysregulated and supports tumor cell proliferation in the context of NF-κB inhibition, we next tested whether the addition of IL-1ra could improve the efficacy of NF-κB inhibitor therapy in two different lung cancer models. In the first model, we injected murine Lewis lung carcinoma (LLC) cells subcutaneously into the flanks of syngeneic WT mice. When tumors reached ~100 mm^2, mice were divided into four treatment groups: bortezomib, IL-1ra, bortezomib plus IL-1ra, or vehicle control. Bortezomib (or vehicle) was administered by i.p. injection twice weekly, and IL-1ra (or PBS control) was administered throughout the treatment course via osmotic pump. Whereas monotherapy with bortezomib or IL-1ra did not affect tumor growth, combination therapy with bortezomib and IL-1ra significantly reduced tumor growth compared to all other groups (Figure 7E). For the second model, we used doxycycline (dox)-inducible Kras^{G12D} mice (Fisher et al., 2001). In a preliminary study, we treated mice with dox for 4 weeks, followed by bortezomib twice weekly for 1 week, and found increased neutrophils in the lungs compared to vehicle-treated mice (Figure 7F). Subsequently, we treated inducible Kras^{G12D} mice with dox for 4 weeks and then randomized mice to treatment with bortezomib, IL-1ra, bortezomib plus IL-1ra, or vehicle control for 4 additional weeks. While treatment with bortezomib reduced tumor numbers compared to vehicle control and IL-1ra groups, lung tumors were reduced by 90% in mice administered combination therapy with bortezomib and IL-1ra (Figures 7G and 7H). In these studies, combination therapy with bortezomib and IL-1ra reduced tumor formation and growth and was more effective than bortezomib alone.

DISCUSSION

Our studies identify IL-1β as a targetable, pro-tumorigenic mediator that contributes to the resistance of lung tumors to NF-κB inhibitors. We showed that inhibition of NF-κB in myeloid cells enhances lung tumorigenesis and, paradoxically, increases infiltration of neutrophils into the lungs. NF-κB-deficient neutrophils produced elevated levels of IL-1β, which was regulated by the serine protease cathepsin G. Consistent with studies in mice with myeloid-specific NF-κB inhibition, systemic delivery of pharmacological NF-κB inhibitors to WT mice significantly increased lung neutrophils and IL-1β production during lung tumorigenesis. In humans with advanced stage NSCLC, plasma IL-1β concentration inversely correlated with progression-free survival, and IL-1β levels were increased following treatment with the proteasome inhibitor bortezomib. Neutrophil depletion studies and pharmacological IL-1ra treatment, both of which reduced lung tumors in the setting of myeloid NF-κB inhibition, support a causative role for neutrophil-derived IL-1β in lung tumorigenesis. Furthermore, we demonstrated that combined treatment with bortezomib and IL-1ra reduces tumor formation and growth in vivo and that IL-1β exerts its pro-tumorigenic effects by stimulating lung epithelial cell proliferation. In addition to demonstrating an important role for IL-1β in promoting lung carcinogenesis and mediating resistance to NF-κB inhibitors, these data support broader utilization of rational combined biological therapies to treat lung cancer.

Together with existing literature, our findings suggest that the lung microenvironment could support both pro- and anti-tumorigenic outcomes resulting from the inhibition of NF-κB signaling. Consistent with our previous studies showing pro-tumorigenic outcomes from long-term bortezomib treatment (Karabela et al., 2012), these data demonstrate that inhibition of NF-κB signaling, specifically in myeloid cells, enhances lung tumorigenesis. Our findings are also in agreement with a recent report in which myeloid NF-κB inhibition supported enhanced growth of melanomas (Yang et al., 2014). In opposition, previous studies using a colon cancer model and a model of lung cancer induced by oncogenic Kras plus cigarette smoke found that inhibition of NF-κB signaling in myeloid cells inhibited tumorigenesis (Greten et al., 2004; Takahashi et al., 2010). We suggest that differences in tumorigenic outcomes in response to myeloid-specific NF-κB inhibition may be due to differential effects on pre-existing inflammation in the tumor microenvironment. Both the model of azoxymethane plus dextran sulfate colon cancer and the model of oncogenic Kras plus cigarette smoke are highly inflammatory models in which myeloid NF-κB inhibition reduces carcinogenesis as well as cytokine expression and inflammatory cell infiltration (Greten et al., 2004; Takahashi et al., 2010). In contrast, the lung cancer models in our studies result in only mild inflammation, and myeloid NF-κB inhibition increases inflammation in these settings. Therefore, it may be that the overall impact of myeloid NF-κB inhibition on tumorigenesis is dependent upon the inflammatory environment. In environments with high levels of pre-existing inflammation, inhibition of NF-κB signaling may reduce pro-tumorigenic inflammation by blocking transcription of NF-κB-dependent mediators, consequently suppressing tumor formation and growth. In contrast, the upregulation of IL-1β processing by neutrophils may play an important pro-tumorigenic role in less inflammatory environments, which may be more similar to human lung cancer, by providing important proliferation signals to mutated epithelial cells. In either case, it may be that a combination of biological approaches to block inflammatory signaling are superior to NF-κB inhibition alone.

In our studies, we discovered that both myeloid-specific and systemic inhibition of NF-κB induce an increase in lung neutrophils during lung carcinogenesis. This increase in lung neutrophils was not a result of increased circulating neutrophils but could be related to increased recruitment or prolonged survival, which has been previously described for NF-κB-inhibited neutrophils (Hsu et al., 2011; Langereis et al., 2010). Although we found increased expression of the neutrophil chemoattractant KC in urethane-treated IKKβ$^{\Delta mye}$ mice, WT mice treated with systemic NF-κB inhibitors also had increased neutrophils in the lungs but did not show increased KC expression, suggesting that KC is not

the critical mediator of lung neutrophilia observed in our models. The N1/N2 neutrophil polarization paradigm has been used to explain anti- or pro-tumorigenic functions of neutrophils (Fridlender et al., 2009). Several studies have shown that N2 tumor-associated neutrophils exert their pro-tumorigenic properties through production of angiogenic factors, matrix-degrading enzymes, and immunosuppression (reviewed in Sionov et al., 2015). In contrast, our studies show that neutrophils with inhibited NF-κB signaling are not highly polarized toward N1 or N2 and are not immunosuppressive. Instead, NF-κB-deficient neutrophils have a unique pro-tumorigenic phenotype characterized by dysregulated processing of the inflammatory mediator IL-1β.

While we identified an important role for neutrophils in accelerating lung tumorigenesis in the context of NF-κB inhibition, other cell types may also contribute to this phenotype. Although not directly tested in our studies, interactions between neutrophils and macrophages may be important for creating a pro-tumorigenic environment in the lungs. This idea is supported by our previous finding that macrophages are important for urethane-induced tumorigenesis (Zaynagetdinov et al., 2011), as well as by a recent study demonstrating that macrophages with inhibited NF-κB signaling are unable to mediate anti-tumor responses against metastatic melanoma cells (Yang et al., 2014). Future studies are necessary to fully elucidate interactions between inflammatory cell types and epithelial cells that regulate lung carcinogenesis.

A connection between elevated IL-1β and lung cancer in humans has been suggested by studies showing that a single-nucleotide polymorphism (-31C-T) in *IL1B* increases IL-1β expression and lung cancer risk (Li and Wang, 2013; Lind et al., 2007). Our studies extend these findings by showing that IL-1β levels in plasma were inversely correlated with progression-free survival of NSCLC patients. Furthermore, we found that plasma IL-1β levels of NSCLC patients increase following NF-κB inhibition with the proteasome inhibitor bortezomib, suggesting that our explanation for resistance to NF-κB inhibitor therapy is relevant to NSCLC patients. Although the mechanisms by which IL-1β impacts lung tumor biology are not fully understood, our findings suggest that IL-1β exerts its pro-tumorigenic effects by promoting the proliferation of lung epithelial cells. Our observations are consistent with a prior report that IL-1β increases proliferation of human NSCLC cells (Wang et al., 2014).

We found that both myeloid-specific and systemic NF-κB inhibition increase IL-1β protein expression in the lungs. Although IL-1β mRNA expression is regulated by the NF-κB pathway (Cogswell et al., 1994), our findings are consistent with previous reports showing that NF-κB inhibition in myeloid cells increases IL-1β processing under conditions of septic shock and acute lung injury (Greten et al., 2007; Hsu et al., 2011; Huang et al., 2011). While IL-1β processing is thought to be primarily regulated by the inflammasome in most cells, serine proteases have been implicated in IL-1β processing by neutrophils (Greten et al., 2007; Guma et al., 2009). Our findings indicate that cathepsin G strongly regulates IL-1β production by neutrophils and that expression of cathepsin G is upregulated in neutrophils with inhibited NF-κB. Therefore, increased neutrophilia in the lungs during NF-κB inhibition and increased processing of pro-IL-1β by cathepsin G in individual neutrophils likely contribute to increased IL-1β production in this setting. Since cathepsin G has been correlated with tumor grade and clinical stage in NSCLC (Maksimowicz et al., 1997), future studies targeting this protease could be warranted.

Although IL-1 receptor blockade alone was ineffective in reducing tumor formation and growth in our models, these studies demonstrate that the addition of IL-1ra to NF-κB inhibition improves the effectiveness of NF-κB inhibitor therapy. In a heterotopic flank tumor model, combination therapy was the only regimen that slowed tumor growth, compared to vehicle control. In the dox-inducible $Kras^{G12D}$ model, bortezomib monotherapy reduced tumor formation, but combination therapy with bortezomib and IL-1ra was most effective. These findings indicate that the effects of bortezomib are variable and model dependent. In contrast, we showed impressive responses to combined bortezomib/IL-1ra treatment in both tumor models tested. Of the 35 clinical trials included in the ClinicalTrials.gov database that investigate bortezomib in lung cancer, only three have used combined therapy with bortezomib and another targeted agent. Since combined targeted therapies may be the most direct way to manage disease and reduce nonspecific side effects from treatment (Gibbs, 2000), our studies support future human studies combining NF-κB inhibitors with IL-1ra or other targeted biological therapies aimed at overcoming resistance mechanisms.

EXPERIMENTAL PROCEDURES

Mouse Studies

All animal care and experimental procedures were approved and conducted according to guidelines issued by the Vanderbilt University Institutional Animal Care and Use Committee. Lung tumors were induced in $IKK\beta^{\Delta mye}$ mice ($IKK\beta^{fl/fl}$; LysM-Cre) (Li et al., 2003) and littermate WT controls by a single i.p. injection of urethane (ethyl carbamate, 1 g/kg) (Sigma-Aldrich). BAY 11-7082 (10 mg/kg body weight; Cayman Chemical) or bortezomib (1 mg/kg; Selleckchem) was delivered by i.p. injection as described previously (Xue et al., 2011). Lung tumors were induced in LSL-$Kras^{G12D}$ mice (Tuveson et al., 2004), using i.t. instillation of adeno-Cre (1.5×10^7 plaque-forming units [PFUs]). Lung tumors were established in mice expressing dox-inducible $Kras^{G12D}$ in $CCSP^+$ lung epithelial cells (CCSP-rtTA (tet-O)- $Kras^{G12D}$) and littermate WT controls (Fisher et al., 2001) via consumption of dox (0.5 g/l) in drinking water for 4 weeks. Subsequently, mice were treated with dox plus vehicle control, bortezomib, IL-1ra (60 mg/kg/day; Amgen), or a combination of bortezomib and IL-1ra for 4 weeks. Subcutaneous tumors in C57BL/6 mice were established by an injection of 2.5×10^5 syngeneic LLC cells in the right flank. When tumor size reached about 100 mm^2, mice were randomized and treated with vehicle control, bortezomib, IL-1ra, or a combination of bortezomib and IL-1ra. Tumor sizes were measured using Traceable digital calipers (Fisher Scientific). NF-κB reporter mice have been previously described (Everhart et al., 2006).

Human Samples

Twenty-eight chemotherapy-naive patients with inoperable locally advanced (stage IIIB) or metastatic (stage IV) NSCLC were treated with bortezomib (1 mg/m^2) as part of a phase-II clinical trial performed at the University Hospital of Crete (Protocol NCT01633645). Bortezomib was administered alone for the first cycle of treatment. All subsequent treatment cycles contained bortezomib plus gemcitabine and cisplatin. Plasma samples were collected before and 24 hr after the first dose of bortezomib. This trial (The "Velcade" project) was approved by the institutional review board (IRB) of the University Hospital of Crete (no. 8433/21-09-2006) and the National Ethics Committee (no. 77659/22-11-2007).

Neutrophil Depletion, Macrophage Depletion, and Neutralization of IL-1 Receptor

For neutrophil depletion, 100 μg of anti-Ly6G antibodies (Clone 1A8, BioLegend) or IgG2a isotype control antibodies (BioLegend) were delivered by i.p. injection twice a week for the first 6 weeks after urethane injection. Depletion of macrophages was conducted as previously described (Zaynagetdinov et al., 2011). To block IL-1β signaling, mice were treated with 60 mg/kg/day of IL-1ra (anakinra/Kineret, Amgen) or PBS (vehicle control) delivered by subcutaneously implanted Alzet osmotic pumps (infusion rate of 0.5 μl/hr, DURECT). After 2 weeks, osmotic pumps were replaced to complete a 4-week course of treatment.

Statistical Analysis

Mouse data were analyzed using the GraphPad Prism 5.0 software (GraphPad Software), and values are presented as mean ± SEM. Pairwise comparisons were made using Student's t tests. For experiments conducted over several time points or with multiple comparisons, a two-way ANOVA with a Bonferroni post-test was used.

Data from the 28 chemotherapy-naive subjects were analyzed using R software version 3.1.2 (www.r-project.org) and were expressed as median (interquartile range) for continuous variables and frequencies (proportions) for categorical variables. IL-1β, IL-8, TNF, and IL-6, before and 24 hr after initial treatment, were compared using Student's t test. Spearman correlation between baseline IL-1β and progression-free survival time in months was analyzed. We further applied a multivariable linear regression model to adjust for both subjects' age at baseline and performance status. Normality of residuals of the linear model was diagnosed, and log transformation on progression-free survival time was performed to correct non-normal residuals, if needed. $p < 0.05$ was considered statistically significant for both mouse and human data.

Further experimental procedures are described in the Supplemental Information.

SUPPLEMENTAL INFORMATION

Supplemental Information includes Supplemental Experimental Procedures, four figures, and two tables and can be found with this article online at http://dx.doi.org/10.1016/j.celrep.2016.05.085.

AUTHOR CONTRIBUTIONS

Conceptualization, A.G.M., R.Z., and T.S.B; Methodology, A.G.M., L.A.G., G.T.S., and R.Z; Investigation, A.G.M., T.P.S., D.-S.C., W.H., J.A.S., L.A.G., P.W., V.V.P., G.T.S., and R.Z.; Writing – Original Draft, A.G.M., R.Z., and T.S.B.; Writing – Review & Editing, A.G.M., G.T.S., F.E.Y., R.Z., and T.S.B.; Funding Acquisition, R.Z., G.T.S., and T.S.B.; Resources, M.K., F.E.Y., and V.G.; Supervision, A.G.M., R.Z., and T.S.B.

ACKNOWLEDGMENTS

This work was supported by a grant from the Lung Cancer Initiative of North Carolina and Free to Breathe (R.Z.), by NIH grant T32HL094296 (R.Z.), by European Research Council Starting Independent Investigator grant FP7-IDEAS-ERC-StG-2010-260524-KRASHIMPE (G.T.S.), by the U.S. Department of Veterans Affairs (T.S.B.), and by a Vanderbilt-Ingram Cancer Center Spore grant 2010 (T.S.B.).

Received: August 8, 2014
Revised: April 26, 2016
Accepted: May 19, 2016
Published: June 16, 2016

REFERENCES

Bassères, D.S., Ebbs, A., Levantini, E., and Baldwin, A.S. (2010). Requirement of the NF-kappaB subunit p65/RelA for K-Ras-induced lung tumorigenesis. Cancer Res. *70*, 3537–3546.

Bassères, D.S., Ebbs, A., Cogswell, P.C., and Baldwin, A.S. (2014). IKK is a therapeutic target in KRAS-Induced lung cancer with disrupted p53 activity. Genes Cancer *5*, 41–55.

Besse, B., Planchard, D., Veillard, A.S., Taillade, L., Khayat, D., Ducourtieux, M., Pignon, J.P., Lumbroso, J., Lafontaine, C., Mathiot, C., and Soria, J.C. (2012). Phase 2 study of frontline bortezomib in patients with advanced non-small cell lung cancer. Lung Cancer *76*, 78–83.

Chen, W., Li, Z., Bai, L., and Lin, Y. (2011). NF-kappaB in lung cancer, a carcinogenesis mediator and a prevention and therapy target. Front. Biosci. (Landmark Ed.) *16*, 1172–1185.

Chen, L.C., Wang, L.J., Tsang, N.M., Ojcius, D.M., Chen, C.C., Ouyang, C.N., Hsueh, C., Liang, Y., Chang, K.P., Chen, C.C., and Chang, Y.S. (2012). Tumour inflammasome-derived IL-1β recruits neutrophils and improves local recurrence-free survival in EBV-induced nasopharyngeal carcinoma. EMBO Mol. Med. *4*, 1276–1293.

Cogswell, J.P., Godlevski, M.M., Wisely, G.B., Clay, W.C., Leesnitzer, L.M., Ways, J.P., and Gray, J.G. (1994). NF-kappa B regulates IL-1 beta transcription through a consensus NF-kappa B binding site and a nonconsensus CRE-like site. J. Immunol. *153*, 712–723.

Enzler, T., Sano, Y., Choo, M.K., Cottam, H.B., Karin, M., Tsao, H., and Park, J.M. (2011). Cell-selective inhibition of NF-κB signaling improves therapeutic index in a melanoma chemotherapy model. Cancer Discov. *1*, 496–507.

Everhart, M.B., Han, W., Sherrill, T.P., Arutiunov, M., Polosukhin, V.V., Burke, J.R., Sadikot, R.T., Christman, J.W., Yull, F.E., and Blackwell, T.S. (2006). Duration and intensity of NF-kappaB activity determine the severity of endotoxin-induced acute lung injury. J. Immunol. *176*, 4995–5005.

Fanucchi, M.P., Fossella, F.V., Belt, R., Natale, R., Fidias, P., Carbone, D.P., Govindan, R., Raez, L.E., Robert, F., Ribeiro, M., et al. (2006). Randomized phase II study of bortezomib alone and bortezomib in combination with docetaxel in previously treated advanced non-small-cell lung cancer. J. Clin. Oncol. *24*, 5025–5033.

Fisher, G.H., Wellen, S.L., Klimstra, D., Lenczowski, J.M., Tichelaar, J.W., Lizak, M.J., Whitsett, J.A., Koretsky, A., and Varmus, H.E. (2001). Induction and apoptotic regression of lung adenocarcinomas by regulation of a K-Ras transgene in the presence and absence of tumor suppressor genes. Genes Dev. *15*, 3249–3262.

Fleming, T.J., Fleming, M.L., and Malek, T.R. (1993). Selective expression of Ly-6G on myeloid lineage cells in mouse bone marrow. RB6-8C5 mAb to granulocyte-differentiation antigen (Gr-1) detects members of the Ly-6 family. J. Immunol. *151*, 2399–2408.

Fong, C.H.Y., Bebien, M., Didierlaurent, A., Nebauer, R., Hussell, T., Broide, D., Karin, M., and Lawrence, T. (2008). An antiinflammatory role for IKKbeta through the inhibition of "classical" macrophage activation. J. Exp. Med. *205*, 1269–1276.

Fridlender, Z.G., and Albelda, S.M. (2012). Tumor-associated neutrophils: friend or foe? Carcinogenesis *33*, 949–955.

Fridlender, Z.G., Sun, J., Kim, S., Kapoor, V., Cheng, G., Ling, L., Worthen, G.S., and Albelda, S.M. (2009). Polarization of tumor-associated neutrophil phenotype by TGF-beta: "N1" versus "N2" TAN. Cancer Cell *16*, 183–194.

Gabrilovich, D.I., and Nagaraj, S. (2009). Myeloid-derived suppressor cells as regulators of the immune system. Nat. Rev. Immunol. *9*, 162–174.

Giannou, A.D., Marazioti, A., Spella, M., Kanellakis, N.I., Apostolopoulou, H., Psallidas, I., Prijovich, Z.M., Vreka, M., Zazara, D.E., Lilis, I., et al. (2015). Mast cells mediate malignant pleural effusion formation. J. Clin. Invest. *125*, 2317–2334.

Gibbs, J.B. (2000). Mechanism-based target identification and drug discovery in cancer research. Science *287*, 1969–1973.

Greten, F.R., Eckmann, L., Greten, T.F., Park, J.M., Li, Z.W., Egan, L.J., Kagnoff, M.F., and Karin, M. (2004). IKKbeta links inflammation and tumorigenesis in a mouse model of colitis-associated cancer. Cell *118*, 285–296.

Greten, F.R., Arkan, M.C., Bollrath, J., Hsu, L.C., Goode, J., Miething, C., Göktuna, S.I., Neuenhahn, M., Fierer, J., Paxian, S., et al. (2007). NF-kappaB is a

negative regulator of IL-1beta secretion as revealed by genetic and pharmacological inhibition of IKKbeta. Cell *130*, 918–931.

Guma, M., Ronacher, L., Liu-Bryan, R., Takai, S., Karin, M., and Corr, M. (2009). Caspase 1-independent activation of interleukin-1beta in neutrophil-predominant inflammation. Arthritis Rheum. *60*, 3642–3650.

Hagemann, T., Lawrence, T., McNeish, I., Charles, K.A., Kulbe, H., Thompson, R.G., Robinson, S.C., and Balkwill, F.R. (2008). "Re-educating" tumor-associated macrophages by targeting NF-kappaB. J. Exp. Med. *205*, 1261–1268.

Hsu, L.C., Enzler, T., Seita, J., Timmer, A.M., Lee, C.Y., Lai, T.Y., Yu, G.Y., Lai, L.C., Temkin, V., Sinzig, U., et al. (2011). IL-1β-driven neutrophilia preserves antibacterial defense in the absence of the kinase IKKβ. Nat. Immunol. *12*, 144–150.

Huang, H.J., Sugimoto, S., Lai, J., Okazaki, M., Yamamoto, S., Krupnick, A.S., Kreisel, D., and Gelman, A.E. (2011). Maintenance of IKKβ activity is necessary to protect lung grafts from acute injury. Transplantation *91*, 624–631.

Karabela, S.P., Psallidas, I., Sherrill, T.P., Kairi, C.A., Zaynagetdinov, R., Cheng, D.S., Vassiliou, S., McMahon, F., Gleaves, L.A., Han, W., et al. (2012). Opposing effects of bortezomib-induced nuclear factor-κB inhibition on chemical lung carcinogenesis. Carcinogenesis *33*, 859–867.

Langereis, J.D., Raaijmakers, H.A.J.A., Ulfman, L.H., and Koenderman, L. (2010). Abrogation of NF-κB signaling in human neutrophils induces neutrophil survival through sustained p38-MAPK activation. J. Leukoc. Biol. *88*, 655–664.

Li, C., and Wang, C. (2013). Current evidences on IL1B polymorphisms and lung cancer susceptibility: a meta-analysis. Tumour Biol. *34*, 3477–3482.

Li, Z.W., Omori, S.A., Labuda, T., Karin, M., and Rickert, R.C. (2003). IKK beta is required for peripheral B cell survival and proliferation. J. Immunol. *170*, 4630–4637.

Lin, Y., Bai, L., Chen, W., and Xu, S. (2010). The NF-kappaB activation pathways, emerging molecular targets for cancer prevention and therapy. Expert Opin. Ther. Targets *14*, 45–55.

Lind, H., Haugen, A., and Zienolddiny, S. (2007). Differential binding of proteins to the IL1B -31 T/C polymorphism in lung epithelial cells. Cytokine *38*, 43–48.

Maksimowicz, T., Chyczewska, E., Chyczewski, L., Nikliński, J., Ostrowska, H., Szyszko, J., and Furman, M. (1997). Activity and tissue localization of cathepsin G in non small cell lung cancer. Rocz. Akad. Med. Bialymst. *42* (*Suppl 1*), 199–216.

Meylan, E., Dooley, A.L., Feldser, D.M., Shen, L., Turk, E., Ouyang, C., and Jacks, T. (2009). Requirement for NF-kappaB signalling in a mouse model of lung adenocarcinoma. Nature *462*, 104–107.

Rajnavolgyi, E., Nagy, L., Galdiero, M.R., Bonavita, E., Barajon, I., Garlanda, C., Mantovani, A., and Jaillon, S. (2013). Tumor associated macrophages and neutrophils in cancer. Immunobiology *218*, 1402–1410.

Saxon, J.A., Sherrill, T.P., Polosukhin, V.V., Sai, J., Zaynagetdinov, R., McLoed, A.G., Gulleman, P.M., Barham, W., Cheng, D.S., Hunt, R.P., et al. (2016). Epithelial NF-κB signaling promotes EGFR-driven lung carcinogenesis via macrophage recruitment. OncoImmunology, Published online March 30, 2016. http://dx.doi.org/10.1080/2162402X.2016.1168549.

Sionov, R.V., Fridlender, Z.G., and Granot, Z. (2015). The multifaceted roles neutrophils play in the tumor microenvironment. Cancer Microenviron. *8*, 125–158.

Stathopoulos, G.T., Sherrill, T.P., Cheng, D.S., Scoggins, R.M., Han, W., Polosukhin, V.V., Connelly, L., Yull, F.E., Fingleton, B., and Blackwell, T.S. (2007). Epithelial NF-kappaB activation promotes urethane-induced lung carcinogenesis. Proc. Natl. Acad. Sci. USA *104*, 18514–18519.

Stathopoulos, G.T., Sherrill, T.P., Karabela, S.P., Goleniewska, K., Kalomenidis, I., Roussos, C., Fingleton, B., Yull, F.E., Peebles, R.S., Jr., and Blackwell, T.S. (2010). Host-derived interleukin-5 promotes adenocarcinoma-induced malignant pleural effusion. Am. J. Respir. Crit. Care Med. *182*, 1273–1281.

Takahashi, H., Ogata, H., Nishigaki, R., Broide, D.H., and Karin, M. (2010). Tobacco smoke promotes lung tumorigenesis by triggering IKKbeta- and JNK1-dependent inflammation. Cancer Cell *17*, 89–97.

Tichelaar, J.W., Zhang, Y., leRiche, J.C., Biddinger, P.W., Lam, S., and Anderson, M.W. (2005). Increased staining for phospho-Akt, p65/RELA and cIAP-2 in pre-neoplastic human bronchial biopsies. BMC Cancer *5*, 155.

Tuveson, D.A., Shaw, A.T., Willis, N.A., Silver, D.P., Jackson, E.L., Chang, S., Mercer, K.L., Grochow, R., Hock, H., Crowley, D., et al. (2004). Endogenous oncogenic K-ras(G12D) stimulates proliferation and widespread neoplastic and developmental defects. Cancer Cell *5*, 375–387.

Wang, L., Zhang, L.F., Wu, J., Xu, S.J., Xu, Y.Y., Li, D., Lou, J.T., and Liu, M.F. (2014). IL-1β-mediated repression of microRNA-101 is crucial for inflammation-promoted lung tumorigenesis. Cancer Res. *74*, 4720–4730.

Westcott, P.M.K., Halliwill, K.D., To, M.D., Rashid, M., Rust, A.G., Keane, T.M., Delrosario, R., Jen, K.Y., Gurley, K.E., Kemp, C.J., et al. (2015). The mutational landscapes of genetic and chemical models of Kras-driven lung cancer. Nature *517*, 489–492.

Xia, Y., Yeddula, N., Leblanc, M., Ke, E., Zhang, Y., Oldfield, E., Shaw, R.J., and Verma, I.M. (2012). Reduced cell proliferation by IKK2 depletion in a mouse lung-cancer model. Nat. Cell Biol. *14*, 257–265.

Xue, W., Meylan, E., Oliver, T.G., Feldser, D.M., Winslow, M.M., Bronson, R., and Jacks, T. (2011). Response and resistance to NF-κB inhibitors in mouse models of lung adenocarcinoma. Cancer Discov. *1*, 236–247.

Yang, J., Hawkins, O.E., Barham, W., Gilchuk, P., Boothby, M., Ayers, G.D., Joyce, S., Karin, M., Yull, F.E., and Richmond, A. (2014). Myeloid IKKβ promotes antitumor immunity by modulating CCL11 and the innate immune response. Cancer Res. *74*, 7274–7284.

You, M., Candrian, U., Maronpot, R.R., Stoner, G.D., and Anderson, M.W. (1989). Activation of the Ki-ras protooncogene in spontaneously occurring and chemically induced lung tumors of the strain A mouse. Proc. Natl. Acad. Sci. USA *86*, 3070–3074.

Zaynagetdinov, R., Sherrill, T.P., Polosukhin, V.V., Han, W., Ausborn, J.A., McLoed, A.G., McMahon, F.B., Gleaves, L.A., Degryse, A.L., Stathopoulos, G.T., et al. (2011). A critical role for macrophages in promotion of urethane-induced lung carcinogenesis. J. Immunol. *187*, 5703–5711.

Zaynagetdinov, R., Stathopoulos, G.T., Sherrill, T.P., Cheng, D.S., McLoed, A.G., Ausborn, J.A., Polosukhin, V.V., Connelly, L., Zhou, W., Fingleton, B., et al. (2012). Epithelial nuclear factor-κB signaling promotes lung carcinogenesis via recruitment of regulatory T lymphocytes. Oncogene *31*, 3164–3176.

Cell Reports, Volume *16*

Supplemental Information

Neutrophil-Derived IL-1β Impairs the Efficacy of NF-κB Inhibitors against Lung Cancer

Allyson G. McLoed, Taylor P. Sherrill, Dong-Sheng Cheng, Wei Han, Jamie A. Saxon, Linda A. Gleaves, Pingsheng Wu, Vasiliy V. Polosukhin, Michael Karin, Fiona E. Yull, Georgios T. Stathopoulos, Vassilis Georgoulias, Rinat Zaynagetdinov, and Timothy S. Blackwell

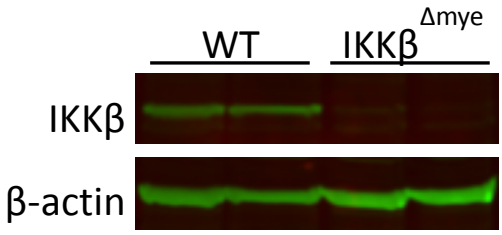

Figure S1 (Related to Figure 1).

Expression of IKKβ protein by western blot in bone marrow cells from WT and IKKβ$^{\Delta mye}$ mice showing deletion of IKKβ in IKKβ$^{\Delta mye}$ mice.

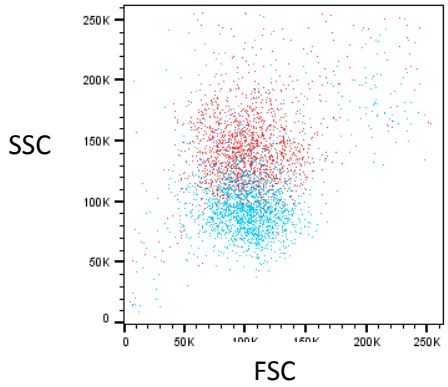

Figure S2 (Related to Figure 2).

FACS plot showing forward scatter (FSC) and side scatter (SSC) of $CD11b^{+}/Gr1^{hi}$ (red) and $CD11b^{+}/Gr1^{low/neg}$ (blue) cells. $CD11b^{+}/Gr1^{hi}$ cells have higher SSC, indicating increased intracellular complexity, which is characteristic of neutrophils.

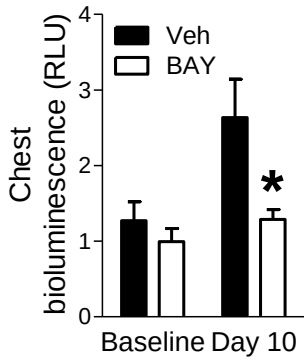

Figure S3 (Related to Figure 6).

BAY 11-7082 treatment blocks NF-κB activation in reporter mice. NF-κB reporter mice were injected with a single dose of urethane and treated with BAY 11-7082 (10 mg/kg by IP injection) or vehicle control 3 times per week. Chest bioluminescence was measured at baseline (prior to urethane treatment) and 10 days after urethane injection (RLU = relative light units). NF-κB reporter mice that express a green fluorescent protein-luciferase fusion protein under control of an NF-κB dependent promoter were injected intravenously with D- luciferin (1 mg) followed by bioluminescent imaging.

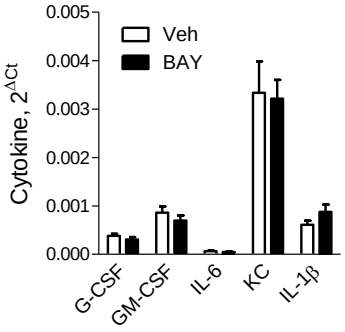

Figure S4 (Related to Figure 6).

Expression of cytokines by mRNA in the lungs of WT mice injected with urethane and treated with BAY 11-7082 (10 mg/kg) or vehicle control (Veh) for 1 week.

Table S1 (Related to Figure 6).

Characteristics of NSCLC patients treated with bortezomib.

Patient Characteristics	**Total (n=28)**
Age, y	75.5 (68.5, 79.2)*
Male gender	22 (78.6%)†
Cancer stage	
IIIB	1 (3.6%)†
IV	27 (96.4%)†
Cancer histology	
Adenocarcinoma	11 (39.3%)†
Squamous	11 (39.3%)†
Other NSCLC	6 (21.4%)†
Performance score	
0	19 (67.9%)†
1	9 (32.1%)†
Progression-free survival, mo	3.6 (1.7, 6.4)*
Overall survival, mo	10.2 (4.7, 21.0)*

*Data are represented as median (interquartile range)

†Data are represented as total (percent)

Supplemental Experimental Procedures

Bronchoalveolar lavage (BAL)

BAL cells were collected and counted as previously described (Stathopoulos et al., 2007).

Histology and immunohistochemistry.
Lung tumors and atypical adenomatous hyperplasia (AAH) lesions were counted as previously described (Zaynagetdinov et al., 2011). For proliferation and apoptosis analyses, lung sections were immunostained with antibodies against PCNA (Life Technologies) or cleaved caspase-3 (Cell Signaling). Proliferation and apoptosis indices were calculated by counting the number of positive cells per 40x field and averaged from 25 randomly chosen fields.

Isolation of lung cells and flow cytometry/FACS
Lung single-cell suspensions were prepared as described (Zaynagetdinov et al., 2011). Cells were stained with the following antibodies: CD45 - APC-Cy7, CD11b - V450, Gr1 - PerCP-Cy5.5 (BioLegend); Ly6C - FITC and Ly6G - PerCP-Cy5.5 (BD Bioscience); MPO – FITC (Abcam). Flow cytometry was performed using the BD LSR II flow cytometer (BD Bioscience). Data were analyzed with FlowJo software (TreeStar). $CD11b^+$ cells were purified by magnetic separation using microbeads (Miltenyi Biotec) followed by FACS based on expression of Ly6G and Ly6C.

Western blot
Whole lung lysates were prepared using CelLytic^{TM} MT Cell Lysis Reagent (C3228; Sigma-Aldrich), separated by SDS-PAGE gel, transferred to nitrocellulose membrane, and probed with the anti-IKKβ (10AG2; Novus Biologicals) and anti-β-actin (A5316; Sigma-Aldrich). Immunodetection was performed using the corresponding AlexaFluor-conjugated antibodies and the Odyssey Infrared Imaging System (LI-COR Biosciences).

Allogenic mixed leukocyte reaction (MLR) assay
Responder $CD4^+/CD25^-$ effector T cells (Teff) from spleens of naive FVB mice ($1x10^5$ per well) were labeled with CFSE (5 mM; Life Technologies) and activated with allogeneic mature bone marrow-derived dendritic cells from C57BL/6 mice. The suppressive function of $CD11b^+/Ly6G^+$ lung neutrophils from $IKK\beta^{\Delta mye}$ mice was tested on the proliferation of CFSE-labeled Teff cells by flow cytometry. Dead cells were excluded from analysis on the basis of staining with DAPI (4-6-Diamidino-2-phenylindole, Life Technologies).

Protein expression
G-CSF, GM-CSF, IFNγ, IL-4, IL-6, IL-10, IL-12p40, KC, MCP-1, and MIP-1α concentrations were measured by the MILLIPLEX MAP Mouse Cytokine/Chemokine Panel (Millipore). Murine IL-1β protein was measured by ELISA (BioLegend). Human plasma IL-1β, IL-6, IL-8, and TNF were measured using the BD^{TM} Cytometric Bead Array Human Enhanced Sensitivity Flex Sets (BD Biosciences).

***In vitro* inhibitor studies**
Equal numbers of cells (0.15×10^6) were seeded into 96-well plates. Cells were cultured for 1 hour in the presence of Ac-YVAD-CMK (100μM; N-1330.0005; Bachem), MeOSuc-APPV-CMK (100μM; CAS 65144-34-5; Santa Cruz Biotechnology), or Z-GLP-CMK (100μM; 03CK00805; MP Biomedicals).

Bone marrow transplantation
Lethally irradiated (9.5 Gy) recipient mice were injected with bone marrow cells (2×10^6 bone marrow cells/mouse in PBS) from sex-matched, syngeneic donor mice. Animals were then housed for eight weeks under specific pathogen free (SPF) conditions with access to acidified water (pH 2.0) containing neomycin (100 mg/L, Sigma-Aldrich) and polymyxin B (10 mg/L, Sigma-Aldrich) from 3 days before transplantation until 14 days after transplantation. Mice were used for studies 8 weeks following transplantation.

Real-time PCR
RNA from lung tissue or sorted myeloid cells was isolated using the RNeasy Mini kit (Qiagen). cDNA was generated using SuperScript III Reverse Transcriptase (Life Technologies) and subjected to Real-Time PCR using SYBR Green PCR Master Mix (Life Technologies). PCR primers are listed below. Relative mRNA expression in each sample was normalized to GAPDH and presented using the comparative Ct method ($2^{\Delta Ct}$).

Table S2. (Related to Figures 4 and 5).

Primer sets used in this study.

Gene	Forward Primer (5'→3')	Reverse Primer (5'→3')
G-CSF	TTGGTGAGTGGGGTTGCCATAGGT	TGCCCTCTTCTCATTTGTGCTCCT
GM-CSF	CGTTGGTGAGTGAGGGAGAGAGTT	TGAAAGGCAGGGCAAGACAAGG
IL-6	AAAGAGTTGTGCAATGGCAATTCT	AAGTGCATCATCGTTGTTCATACA
KC	CCGAAGTCATAGCCACACTCAA	GCAGTCTGTCTTCTTTCTCCGTTAC
IL-1β	GCAACTGTTCCTGAACTCAACT	ATCTTTTGGGGTCCGTCAACT
CatG	GCCAATCGCTTCCAGTTCTAC	GTGGGTGTTCACATTCTTACCC
TNFα	AAGCCTGTAGCCCACGTCGTA	GGCACCACTAGTTGGTTGTCTTTG
IL-12p35	TGGACCTGCCAGGTGTCTTAG	CAATGTGCTGGTTTGGTCCC
ICAM1	TGCCTCTGAAGCTCGGATATAC	TCTGTCGAACTCCTCAGTCAC
IFNγ	GCGTCATTGAATCACACCTGA	CTCGGATGAGCTCATTGAATGC
iNOS	CACCTTGGAGTTCACCCAGT	ACCACTCGTACTTGGGATGC
CCL2	TTAAAAACCTGGATCGGAACCAA	GCATTAGCTTCAGATTTACGGGT
CCL5	ACCATGAAGATCTCTGCAGC	TGAACCCACTTCTTCTCTGG
CCL17	TGCTTCTGGGGACTTTTCTG	CATCCCTGGAACACTCCACT
VEGF	TTACTGCTGTACCTCCACC	ACAGGACGGCTTGAAGATG
IL-10	ACCTGCTCCACTGCCTTGCT	GGTTGCCAAGCCTTATCGGA
Arg1	GATTGGCAAGGTGATGGAAG	TCAGTCCCTGGCTTATGGTT
GAPDH	TGAGGACCAGGTTGTCTCCT	CCCTGTTGCTGTAGCCGTAT